

ISCI, Volume 21

## Supplemental Information

### Plant-Derived Exosomal

### Nanoparticles Inhibit Pathogenicity

### of *Porphyromonas gingivalis*

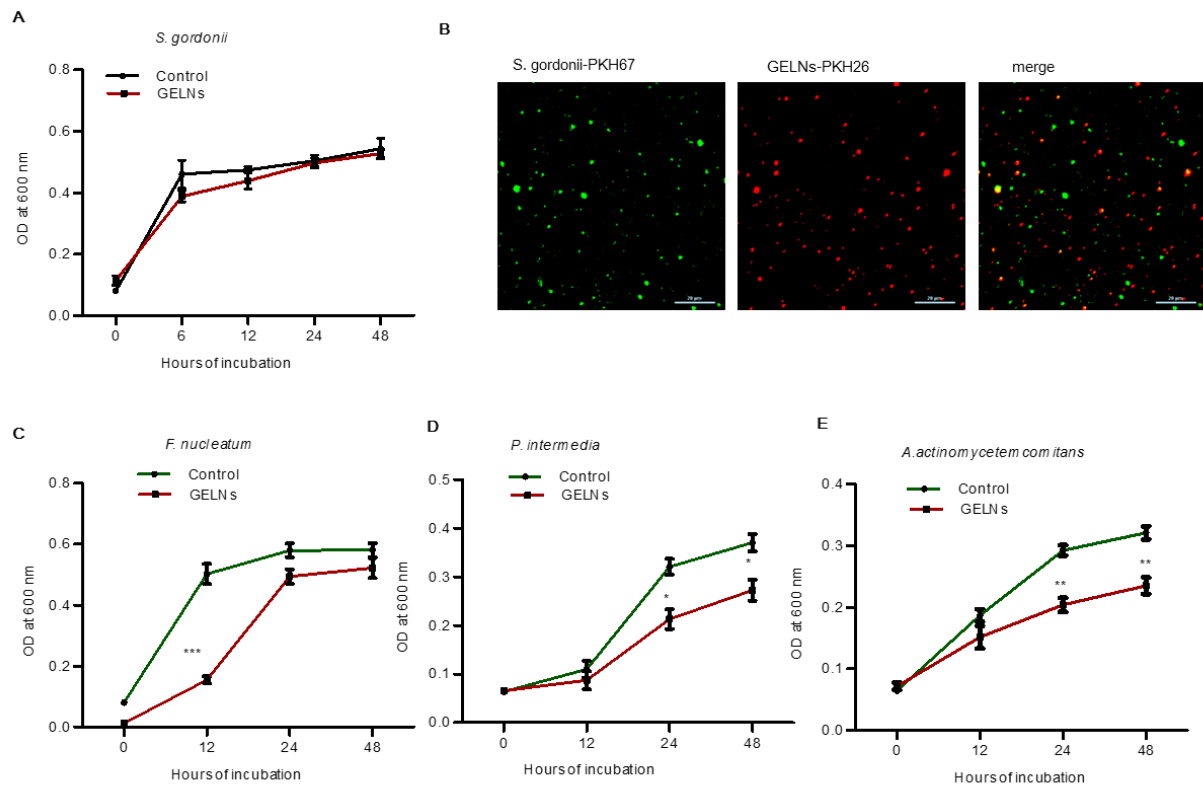
Kumaran Sundaram, Daniel P. Miller, Anil Kumar, Yun Teng, Mohammed Sayed, Jingyao Mu, Chao Lei, Mukesh K. Sriwastva, Lifeng Zhang, Yan Jun, Michael L. Merchant, Liqing He, Yuan Fang, Shuangqin Zhang, Xiang Zhang, Juw W. Park, Richard J. Lamont, and Huang-Ge Zhang

## **Supplemental Information**

### **Plant-Derived Exosomal Nanoparticles Inhibit Pathogenicity of *Porphyromonas gingivalis***

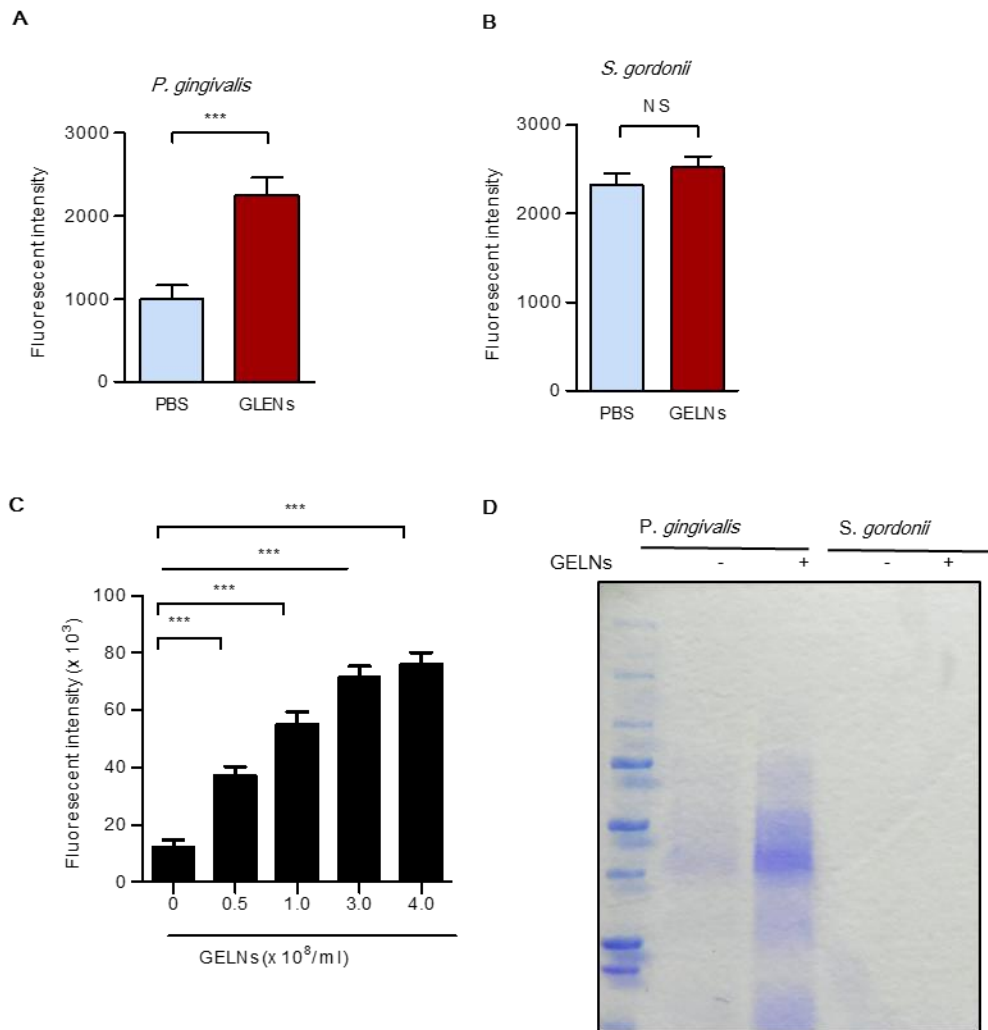
**Kumaran Sundaram, Daniel P. Mille, Anil Kumar , Yun Teng, Mohammed Sayed, Jingyao Mu, Chao Lei, Mukesh K Sriwastva, Lifeng Zhang, Yan Jun, Michael L Merchant, Liqing He, Yuan Fang, Shuang Qin Zhang, Xiang Zhang, Juw Won Park, Richard J. Lamont, and Huang-Ge Zhang**

**Figure S1. GELNs did not affect the growth of *S. gordonii*, Related to Figure 1.**



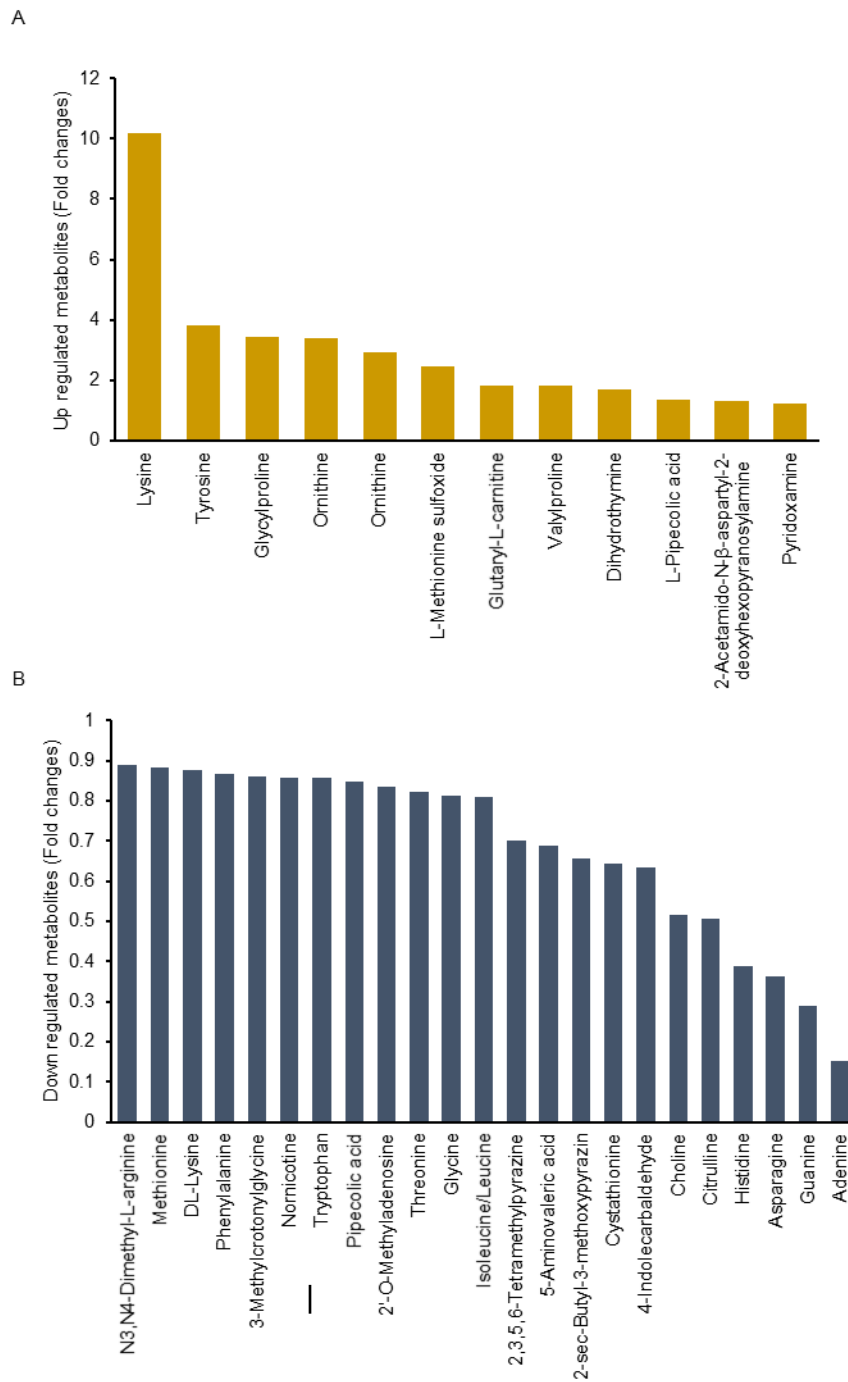
**(A)** *S. gordonii* was treated with GELNs ( $4.0 \times 10^8/\text{ml}$ ) for the indicated times. **(B)** *S. gordonii* did not take up GELNs. *S. gordonii* and GELNs were labelled with fluorescent dyes PKH67 and PKH26, respectively. *S. gordonii* was incubated with GELNs for 1 h at  $37^\circ\text{C}$ . Uptake of GELNs by *S. gordonii* was determined using confocal microscopy. **(C-E)** *F. nucleatum*, *P. intermedia* and *A. actinomycetemcomitans* was treated with GELNs ( $4.0 \times 10^8/\text{ml}$ ) for the indicated times. The growth of *S. gordonii* was determined by measuring optical density at 600 nm. Results are expressed as mean  $\pm$  standard deviation from three independent experiments. \* $P < 0.05$ , \*\* $P < 0.01$ , \*\*\* $P < 0.001$  compared with an untreated group using a one-way ANOVA with the Turkey's Multiple Comparison Test.

**Figure S2. GELNs modulate inner membrane depolarization and membrane fluidity in *P. gingivalis*, Related to Figure 1.**



**(A-B)** *P. gingivalis* and *S. gordonii* were washed with HEPES–glucose buffer and incubated with 0.4  $\mu$ M of diSC3-5 for 1 h. Bacteria were treated with GELNs ( $6.0 \times 10^8$  particles /ml) for 2 h. Membrane depolarization was measured by fluorescence intensity at 620 nm excitation and 722 nm emission. **(C)** *P. gingivalis* was incubated with different concentrations (0– $6.0 \times 10^8$  particles /ml) of GELNs for 2 h at 37°C and 0.5  $\mu$ M of ethidium bromide was added. The fluorescent intensity was measured at 540 nm and 610 nm of excitation and emission, respectively. **(D)** *P. gingivalis* and *S. gordonii* were treated with GELNs ( $4.0 \times 10^8$  particles /ml) for 24 h and centrifuged (10,000 rpm) for 10 min to remove bacteria. The supernatant was separated by SDS-PAGE and stained with Coomassie brilliant blue. Results are expressed as means  $\pm$  standard deviation from three independent experiments. NS; Not significant, \*\*\* $P < 0.001$  compared with an untreated control group using Student 't' Test.

**Figure S3. GELNs modulate metabolic pathways in *P. gingivalis*, Related to Figure 1.**

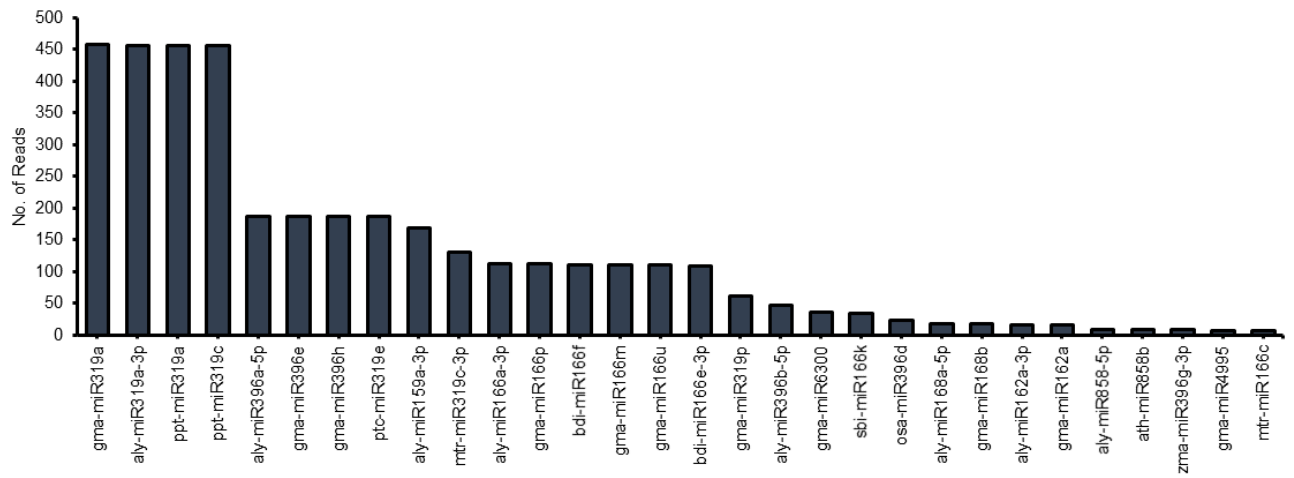


*P. gingivalis* was treated with GELNs ( $4 \times 10^8$  particles /ml) for 24 h. Metabolic product in the supernatant were measured by LC- MS. **(A)** upregulated metabolic products. **(B)** down regulated metabolic products.

**Table S1: Metabolies released by *P. gingivalis* released metabolites and their function, Related to Figure 1.**

<b>Metabolites</b>	<b>Function</b>	<b>Reference</b>
Lysine	lysine, is required in protein synthesis and in the peptidoglycan layer of Gram-positive bacterial cell walls	(Gillner et al., 2013)
Tyrosine	D-tyrosine has potent activity toward biofilm disassembly	(Kolodkin-Gal et al., 2010)
Proline	Protection against abiotic stress, osmoregulation, protein stability, involved in cell signaling and energy production	(Christgen and Becker, 2018)
Ornithine	contribute to cytosolic pH homeostasis when cells are exposed to acidic environments	(Viala et al., 2011)
L- methionine sulfoxide	Defends against oxidative stress	(Luo and Levine, 2009)
L-Carnitine	Role in electron transport chain, osmoprotection, served as nutrient	(Meadows and Wargo, 2015)
L-pipecolic acid	served as carbon and nitrogen source	(Rao and Rodwell, 1962)
Pyridoxamine	Serves as cofactor of enzymes, role in amino acid and fatty acid metabolism	(El Qaidi et al., 2013)
Dimethyl -L-arginine	Involved in several metabolic pathway and role in bacterial pathogenesis	(Xiong et al., 2016)
Methionine	Initiation of translation, it is common cofactor	(Ferla and Patrick, 2014)
Phenylalanine	Degradation by several anaerobic bacteria and important for growth	(Fuchs et al., 2011)
3-Methylcrotonglycine	Modulates mitochondrial energy production and inhibit ATPase	(Moura et al., 2012)
2'-Methyladenosine	Involved in gene regulation	(Deng et al., 2015)
Threonine	Phosphorylation of protein which play an important role in pathogenesis, host cell interaction	(Cozzone, 2005)
Glycine	Inhibit bacterial growth, inhibit synthesis peptidoglycan on bacterial cell wall	(Hammes et al., 1973)
Isoleucine	Role in bacterial growth	(Conner and Hansen, 1967)
Tetramethylpyrazine	Bacteria used for carbon and energy source	(Kutanovas et al., 2013)
5-Aminovaleric acid	Bacterial catabolic product of Lysine and play a role in biotransformation	(Liu et al., 2014)
Cystathionine	Metabolites used for methionine biosynthesis	(Delavier-Klutchko and Flavin, 1965)
4-Indolecarbaldehyde	Biofilm formation, virulence factor production, antibiotic resistance.	(Melander et al., 2014)
Choline	It is precursor to GB, and GB act as a potent osmoprotectant and roles in shaping microbial communities	(Wargo, 2013)
Citruline	Protects bacteria from acid stress	(Cusumano and Caparon, 2015)
Histidine	Used as a source of carbon, energy, and nitrogen	(Bender, 2012)
Asparagine	Important role in glycoprotein biosynthesis	(Hart, 1982)
Guanine	Bacterial genomic DNA	(Muto and Osawa, 1987)
Adenine	Adenine Methylation play a role in Regulating Bacterial Gene Expression and Virulence	

**Figure S4. miRNA profile of GELNs, Related to Figure 2.**



Total miRNA was extracted from the GELNs and the miRNA profile was determined as described in the Materials and Methods.

**Table S2: GELN-derived miRNA targeting *P. gingivalis* gene, Related to Figure 2.****Aly-miR-159a-3p**

<b>miRNA seed</b>	<b>Gene symbol</b>	<b>locus tag</b>	<b>Description</b>
TTTGGATT	PGN_RS08230	PGN_1733	hemagglutinin
TTTGGATT	PGN_RS05900	PGN_1227	hypothetical protein
TTTGGATT	PGN_RS06005	PGN_1253	hypothetical protein
TTTGGATT	PGN_RS05790	PGN_1204	aspartate 1-decarboxylase
TTTGGATT	PGN_RS04300	PGN_0902	anaphase-promoting protein subunit 3
TTTGGATT	PGN_RS05310		hypothetical protein
TTTGGATT	PGN_RS08315	PGN_1750	3-deoxy-manno-octulosonate cytidyltransferase
TTTGGATT	PGN_RS02060	PGN_0433	phosphoglycerate kinase
TTTGGATT	PGN_RS03450	PGN_0723	succinate-semialdehyde dehydrogenase
TTTGGATT	PGN_RS01525	PGN_0318	precorrin-3B C(17)-methyltransferase
TTTGGATT	PGN_RS04735	PGN_0988	hypothetical protein
TTTGGATT	PGN_RS07385	PGN_1549	ATP-dependent Clp protease proteolytic subunit
TTTGGATT	PGN_RS03750	PGN_0786	hypothetical protein
TTTGGATT	PGN_RS06440	PGN_1349	S9 family peptidase
TTTGGATT	PGN_RS09345	PGN_1976	hypothetical protein
TTTGGATT	PGN_RS02890	PGN_0606	glucosamine-6-phosphate deaminase
TTTGGATT	PGN_RS03215	PGN_0675	thiazole biosynthesis protein ThiJ
TTTGGATT	PGN_RS04470	PGN_0935	hypothetical protein
TTTGGATT	PGN_RS07600	PGN_1594	DNA topoisomerase IV subunit B
TTTGGATT	PGN_RS03485	PGN_0732	hypothetical protein
TTTGGATT	PGN_RS08125	PGN_1708	magnesium chelatase
TTTGGATT	PGN_RS00715	PGN_0152	T9SS C-terminal target domain-containing protein
TTTGGATT	PGN_RS00200	PGN_0043	cell division protein FtsH
TTTGGATT	PGN_RS00390	PGN_0082	AraC family transcriptional regulator
TTTGGATT	PGN_RS06580	PGN_1381	alanine--tRNA ligase
TTTGGATT	PGN_RS00600	PGN_0128	hypothetical protein
TTTGGATT	PGN_RS05340	PGN_1115	hemagglutinin
TTTGGATT	PGN_RS00370	PGN_0079	hypothetical protein
TTTGGATT	PGN_RS04995	PGN_1042	cytochrome D ubiquinol oxidase subunit II
TTTGGATT	PGN_RS02750		mobilization protein
TTTGGATT	PGN_RS05560	PGN_1159	anaphase-promoting protein subunit 3
TTTGGATT	PGN_RS09285	PGN_1963	hypothetical protein
TTTGGATT	PGN_RS00415	PGN_0087	hypothetical protein
TTTGGATT	PGN_RS01490	PGN_0311	DUF4271 domain-containing protein
TTTGGATT	PGN_RS04225	PGN_0884	organic solvent tolerance protein OstA
TTTGGATT	PGN_RS09490	PGN_2005	hypothetical protein
TTTGGATT	PGN_RS00890	PGN_0192	membrane protein
TTTGGATT	PGN_RS09325	PGN_1970	peptidase C25
TTTGGATT	PGN_RS09955	PGN_1340	hypothetical protein
TTTGGATT	PGN_RS01395	PGN_0291	VWA domain-containing protein



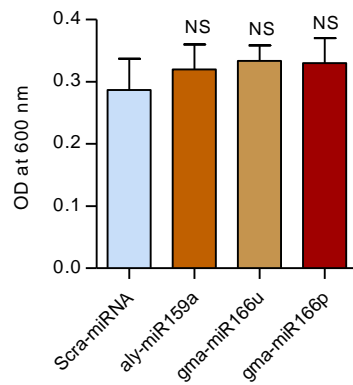
**gma-miR166u**

<b>miRNA_seed</b>	<b>Gene symbol</b>	<b>locus_tag</b>	<b>Description</b>
TCTCGGAC	PGN_RS04795	PGN_1001	DNA polymerase III subunit delta
TCTCGGAC	PGN_RS00800	PGN_0172	hypothetical protein
TCTCGGAC	PGN_RS05480	PGN_1143	hypothetical protein
TCTCGGAC	PGN_RS05135	PGN_1070	radical SAM protein
TCTCGGAC	PGN_RS06355	PGN_1330	branched-chain amino acid ABC transporter ATP-binding protein
TCTCGGAC	PGN_RS07035	PGN_1475	5'-methylthioadenosine/S-adenosylhomocysteine nucleosidase
TCTCGGAC	PGN_RS05385	PGN_1124	paraslipin
TCTCGGAC	PGN_RS06240	PGN_1305	N-acetylmuramoyl-L-alanine amidase
TCTCGGAC	PGN_RS09395	PGN_1986	histidinol phosphate phosphatase
TCTCGGAC	PGN_RS07020	PGN_1471	membrane protein
TCTCGGAC	PGN_RS03965	PGN_0831	transcription antitermination factor NusB
TCTCGGAC	PGN_RS00960	PGN_0205	AraC family transcriptional regulator
TCTCGGAC	PGN_RS08890	PGN_1874	3-phosphoshikimate 1-carboxyvinyltransferase
TCTCGGAC	PGN_RS00680	PGN_0144	DUF5103 domain-containing protein
TCTCGGAC	PGN_RS02140	PGN_0446	ABC transporter ATP-binding protein
TCTCGGAC	PGN_RS03390	PGN_0710	indolepyruvate ferredoxin oxidoreductase
TCTCGGAC	PGN_RS05550	PGN_1157	lysine--tRNA ligase
TCTCGGAC	PGN_RS04840	PGN_1011	adenine permease
TCTCGGAC	PGN_RS00735	PGN_0157	2-iminoacetate synthase ThiH
TCTCGGAC	PGN_RS00090	PGN_0017	sodium-independent anion transporter
TCTCGGAC	PGN_RS03905	PGN_0817	penicillin-binding protein 1A
TCTCGGAC	PGN_RS09895	PGN_2083	potassium transporter
TCTCGGAC	PGN_RS00980	PGN_0209	glycine--tRNA ligase
TCTCGGAC	PGN_RS01460	PGN_0303	peptidase M16
TCTCGGAC	PGN_RS09845	PGN_2075	excinuclease ABC subunit A
TCTCGGAC	PGN_RS02640	PGN_0556	cobaltochelatase
TCTCGGAC	PGN_RS09725	PGN_2050	helicase UvrD

**gma-miR166p**

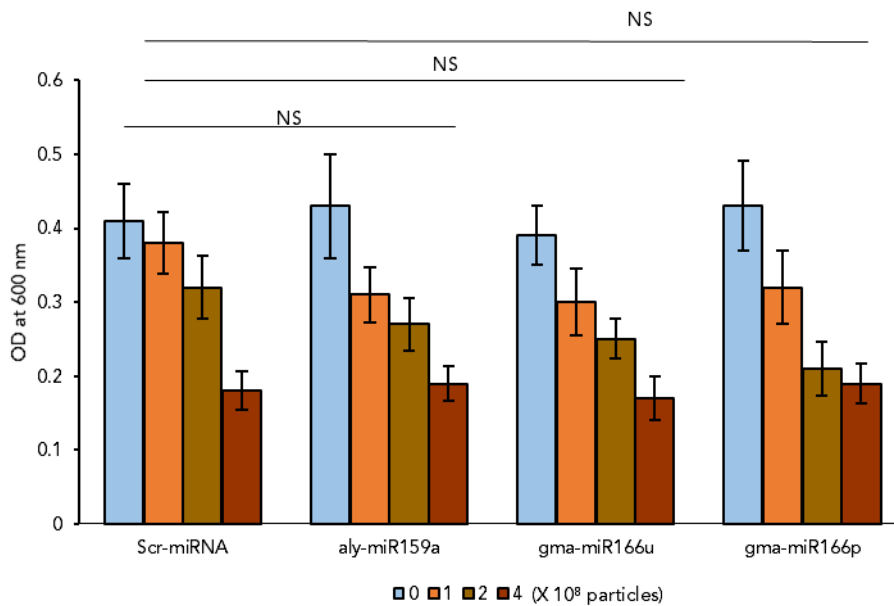
<b>miRNA_seed</b>	<b>Gene symbol</b>	<b>locus_tag</b>	<b>Description</b>
TCGGACCA	PGN_RS01275	PGN_0264	signal recognition particle-docking protein FtsY
TCGGACCA	PGN_RS01430	PGN_0299	outer membrane protein assembly factor
TCGGACCA	PGN_RS03345	PGN_0701	beta-galactosidase

**Figure S5. miRNA from GELNs did not affect the growth of *P.gingivalis*, Related to Figure 2.**



miRNAs aly-miR-159a, gma-miR166u or gma-miR-166p were packaged into lipid nanoparticles and incubated with *P. gingivalis* for 24 h. The growth of *P. gingivalis* was determined by measuring the optical density at 600 nm. Results are expressed as mean  $\pm$  standard deviation from three independent experiments. NS; not significant compared with an scrambled miRNA transduced group using Student 't' Test.

**Figure S6. miRNA and lipids from GLENS have independent roles in *P. gingivalis* growth, Related to Figure 2.**



*P. gingivalis* was transduced with scrambled miRNA, aly-miR159a, gma-miR166u or gma-miR166p or treated with total lipids extracted from different concentrations of GLENS (0- 4.0 × 10<sup>8</sup> particles) and incubated for 24 h. The growth of *P. gingivalis* was measured by optical density at 600 nm. Results are expressed as means with standard deviation from three independent experiments. NS; Not significant represents the comparison of each miRNA with Scr-miRNA with lipid treatment by two-way ANOVA.

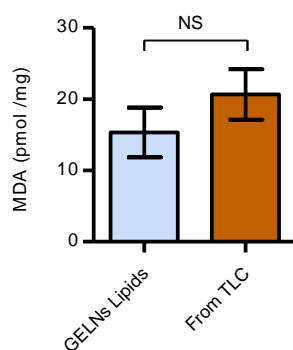
**Table S3: Lipid profile of GELNs, Related to Figure 2.**

Mass	Compound Formula	Compound Name	nmol per mg dry wt
<b>DGDG</b>			
958.6	C51H88O15	DGDG(36:4)	138.65
960.6	C51H90O15	DGDG(36:3)	119.80
936.6	C49H90O15	DGDG(34:1)	97.43
962.6	C51H92O15	DGDG(36:2)	57.25
934.6	C49H88O15	DGDG(34:2)	42.90
956.6	C51H86O15	DGDG(36:5)	29.63
964.7	C51H94O15	DGDG(36:1)	22.88
984.6	C53H90O15	DGDG(38:5)	7.44
932.6	C49H86O15	DGDG(34:3)	5.58
954.6	C51H84O15	DGDG(36:6)	4.87
<b>MGDG</b>			
796.6	C45H78O10	MGDG(36:4)	286.61
794.5	C45H76O10	MGDG(36:5)	170.49
798.6	C45H80O10	MGDG(36:3)	153.29
792.5	C45H74O10	MGDG(36:6)	91.86
800.6	C45H82O10	MGDG(36:2)	33.08
774.6	C43H80O10	MGDG(34:1)	19.13
826.6	C47H84O10	MGDG(38:3)	13.98
772.6	C43H78O10	MGDG(34:2)	9.17
<b>PG</b>			
768.5	C40H79O10P	PG(34:0)	3.71
766.5	C40H77O10P	PG(34:1)	3.30
764.5	C40H75O10P	PG(34:2)	3.11
740.5	C38H75O10P	PG(32:0)	2.23
788.5	C42H75O10P	PG(36:4)	1.82
<b>LysoPG</b>			
526.3	C24H45O9P	LPG(18:2)	26.75
528.3	C24H47O9P	LPG(18:1)	20.15
500.3	C22H43O9P	LPG(16:1)	15.72
502.3	C22H45O9P	LPG(16:0)	14.98
524.3	C24H43O9P	LPG(18:3)	11.47
<b>LysoPC</b>			
520.3	C26H50O7PN	LPC(18:2)	8.32
522.3	C26H52O7PN	LPC(18:1)	5.67
<b>LysoPE</b>			
478.3	C23H44O7PN	LPE(18:2)	1.27
454.3	C21H44O7PN	LPE(16:0)	0.43
452.3	C21H42O7PN	LPE(16:1)	0.37
<b>PC</b>			
758.6	C42H80O8PN	PC(34:2)	7.79
782.6	C44H80O8PN	PC(36:4)	4.77
784.6	C44H82O8PN	PC(36:3)	2.48
760.6	C42H82O8PN	PC(34:1)	2.32
786.6	C44H84O8PN	PC(36:2)	1.08
756.5	C42H78O8PN	PC(34:3)	0.93
780.5	C44H78O8PN	PC(36:5)	0.78
<b>PE</b>			
716.5	C39H74O8PN	PE(34:2)	1.92

740.5	C41H74O8PN	PE(36:4)	1.44
742.5	C41H76O8PN	PE(36:3)	0.22
828.6	C47H90O8PN	PE(42:2)	0.21
718.5	C39H76O8PN	PE(34:1)	0.20
PI			
852.5	C43H79O13P	PI(34:2)	16.28
876.5	C45H79O13P	PI(36:4)	7.98
854.5	C43H81O13P	PI(34:1)	4.37
878.5	C45H81O13P	PI(36:3)	4.08
850.5	C43H77O13P	PI(34:3)	3.44
824.5	C41H75O13P	PI(32:2)	2.65
874.5	C45H77O13P	PI(36:5)	2.50
828.5	C41H79O13P	PI(32:0)	1.99
822.5	C41H73O13P	PI(32:3)	1.91
PS			
872.6	C48H90O10PN	PS(42:2)	8.61
760.5	C40H74O10PN	PS(34:2)	2.75
844.6	C46H86O10PN	PS(40:2)	1.61
900.7	C50H94O10PN	PS(44:2)	1.35
874.6	C48H92O10PN	PS(42:1)	0.93
870.6	C48H88O10PN	PS(42:3)	0.64
786.5	C42H76O10PN	PS(36:3)	0.54
784.5	C42H74O10PN	PS(36:4)	0.49
PA			
690.5	C37H69O8P	PA(34:2)	325.56
714.5	C39H69O8P	PA(36:4)	219.54
716.5	C39H71O8P	PA(36:3)	130.51
692.5	C37H71O8P	PA(34:1)	70.04
718.5	C39H73O8P	PA(36:2)	39.98
688.5	C37H67O8P	PA(34:3)	20.51
712.5	C39H67O8P	PA(36:5)	19.07
666.5	C35H69O8P	PA(32:0)	2.43
DAG			
34:2	C37H72O5N	18:2/16:0	68810.79
34:1	C37H74O5N	18:1/16:0	12404.35
36:4	C39H72O5N	18:2/18:2	7971.51
34:3	C37H70O5N	18:3/16:0	7154.70
36:3	C39H74O5N	18:2/18:1	5916.98
36:2	C39H76O5N	18:2/18:0	1695.15
36:4	C39H72O5N	18:3/18:1	1688.38
36:5	C39H70O5N	18:3/18:2	1203.29
36:2	C39H76O5N	18:1/18:1	1163.96
34:3	C37H70O5N	18:2/16:1	401.01
32:0	C35H72O5N	16:0/16:0	365.18
36:1	C39H78O5N	18:1/18:0	251.94
36:3	C39H74O5N	18:3/18:0	124.73
34:2	C37H72O5N	18:1/16:1	118.98
32:1	C35H70O5N	16:0/16:1	118.12
34:7-O	C37H62O6N	18:3/dnOPDA	82.71
34:4	C37H68O5N	18:2/16:2	82.62
36:6	C39H68O5N	18:3/18:3	79.35
34:4	C37H68O5N	18:3/16:1	52.67

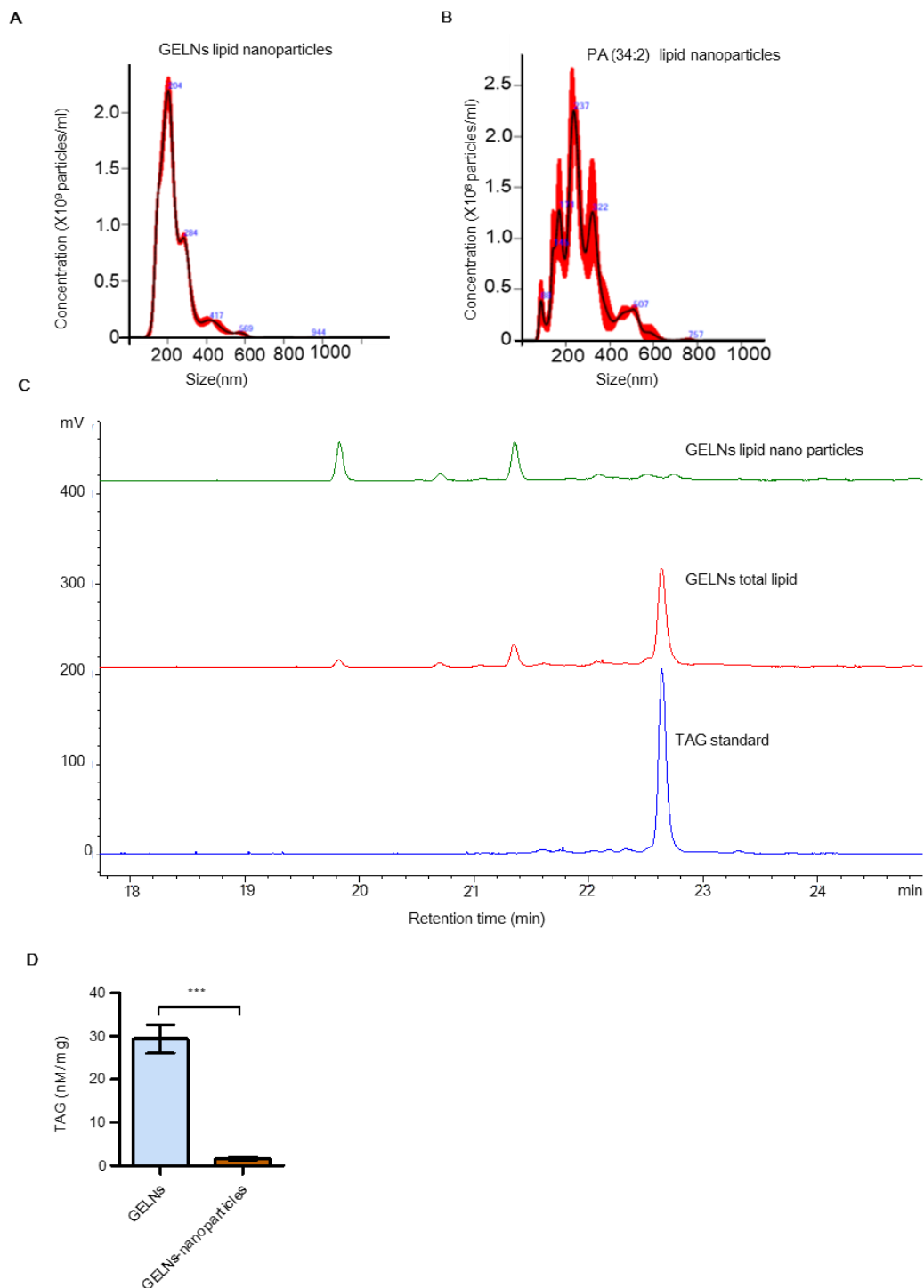
34:5	C37H66O5N	18:2/16:3	40.19
34:3	C37H70O5N	18:1/16:2	34.97
36:7-O	C39H66O6N	OPDA/18:3	22.89
34:1	C37H74O5N	18:0/16:1	15.23
34:2	C37H72O5N	18:0/16:2	15.02
34:6	C37H64O5N	18:3/16:3	13.84
34:4	C37H68O5N	18:1/16:3	13.17
34:7-O	C37H62O6N	OPDA/16:3	11.43
34:5	C37H66O5N	18:3/16:2	9.84
34:8-2O	C37H60O7N	OPDA/dnOPDA	4.68
34:3	C37H70O5N	18:0/16:3	4.61
TAG			
896.76807	C57H102O6N	TAG(54:6)	7.01
894.75247	C57H100O6N	TAG(54:7)	2.91
898.78367	C57H104O6N	TAG(54:5)	2.70
872.76807	C55H102O6N	TAG(52:4)	2.52
894.75247	C57H100O6N	TAG(54:7)	1.86
898.78367	C57H104O6N	TAG(54:5)	1.76
872.76807	C55H102O6N	TAG(52:4)	1.56
896.76807	C57H102O6N	TAG(54:6)	0.98
896.76807	C57H102O6N	TAG(54:6)	0.97
892.73687	C57H98O6N	TAG(54:8)	0.82
900.79927	C57H106O6N	TAG(54:4)	0.81
870.75247	C55H100O6N	TAG(52:5)	0.63
874.78367	C55H104O6N	TAG(52:3)	0.62
874.78367	C55H104O6N	TAG(52:3)	0.61
874.78367	C55H104O6N	TAG(52:3)	0.54
900.79927	C57H106O6N	TAG(54:4)	0.53
848.76807	C53H102O6N	TAG(50:2)	0.50
870.75247	C55H100O6N	TAG(52:5)	0.42
892.73687	C57H98O6N	TAG(54:8)	0.36
848.76807	C53H102O6N	TAG(50:2)	0.23
872.76807	C55H102O6N	TAG(52:4)	0.23
898.78367	C57H104O6N	TAG(54:5)	0.22
850.78367	C53H104O6N	TAG(50:1)	0.19
872.76807	C55H102O6N	TAG(52:4)	0.19
894.75247	C57H100O6N	TAG(54:7)	0.17
876.79927	C55H106O6N	TAG(52:2)	0.17
902.81487	C57H108O6N	TAG(54:3)	0.16
900.79927	C57H106O6N	TAG(54:4)	0.13

**Figure S7. Measurement of lipid oxidation, Related to Figure 2.**



Lipid oxidation of GELNs total lipids and lipids extracted from TLC was measured by level of malondialdehyde (MDA). The lipid sample was mixed with TBA reagent and kept at boiling water bath for 15 min and read at 535 nm. The concentration of MDA was calculated by standard MDA. Results are expressed as mean  $\pm$  standard deviation from three independent experiments. Student 't' Test was used for analysis of statistical significance. NS; Not significant.

**Figure S8. Characterization of GELNs lipid nano particles, Related to Figure 3.**



Lipid nanoparticles were made from LipidG and PA (34:2). Size distribution lipid nanoparticles were determined using a NanoSight NS300 (Westborough, MA) with a flow speed at 0.03 mL per min. **(A)** size distribution of GELNs lipid nanoparticles. **(B)** size distribution of PA (34:2) lipid nanoparticles. **(C-D)** TAG content in GELNs lipid nanoparticles was determined by HPLC. TAG levels were expressed as mean  $\pm$  standard deviation from three independent experiments. Student 't' test was used to analysis statistical significance of TAG level between GELNs total lipid vs GELNs lipid nanoparticles.\*\*\*P<0.001.



**Table S5. GELN-binding proteins of *P. gingivalis*, Related to Figure 5.**

<b>Identified Proteins</b>	<b>Gene Symbol</b>	<b>Accession Number</b>	<b>Molecular Weight</b>
Lys-gingipain	<i>kgp</i>	KGP_PORG3	187 kDa
Hemagglutinin	<i>hagA</i>	B2RLK7_PORG3	283 kDa
Receptor antigen B	<i>ragB</i>	B2RHG8_PORG3	57 kDa
Cluster of Gingipain R1	<i>rgpA</i>	CPG1_PORG3	185 kDa
Receptor antigen A	<i>ragA</i>	B2RHG7_PORG3	115 kDa
35 kDa hemin binding protein	<i>HBP35</i>	B2RII3_PORG3	38 kDa
Peptidylarginine deiminase	PGN_0898	B2RJ72_PORG3	62 kDa
Immunoreactive 61 kDa antigen	<i>tapA</i>	B2RH26_PORG3	61 kDa
C-terminal domain of Arg-and Lys-gingipain proteinase	<i>rgpA_4</i>	B2RHG9_PORG3	32 kDa
Uncharacterized protein	PGN_0654	B2RII8_PORG3	35 kDa
Zn-carboxypeptidase	<i>scpD</i>	B2RHK9_PORG3	92 kDa
Minor fimbrial subunit Mfa1	<i>mfa1</i>	MFA1_PORG3	61 kDa
T9SS C-terminal target domain-containing protease	PGN_0458	B2RHY2_PORG3	57 kDa
Glyceraldehyde-3-phosphate dehydrogenase	<i>gapA</i>	B2RH47_PORG3	36 kDa
NAD-specific glutamate dehydrogenase	<i>gdh</i>	DHE2_PORG3	49 kDa
Uncharacterized protein	PGN_0129	B2RH03_PORG3	22 kDa
Outer membrane lipoprotein immunoreactive 42 kDa antigen PG33	<i>ompA_3</i>	B2RIQ3_PORG3	43 kDa
Fibronectin type III domain protein	<i>fib3</i>	B2RIW9_PORG3	79 kDa
UDP-N-acetylenolpyruvoylglucosamine reductase inner membrane lipoprotein	PGN_1129	B2RJV3_PORG3	17 kDa
Lipoprotein	PGN_0426	B2RHV0_PORG3	17 kDa
Lysyl endopeptidase	<i>pepK</i>	B2RKP0_PORG3	103 kDa
Outer membrane lipoprotein immunoreactive 42 kDa antigen PG33	<i>ompA_2</i>	B2RIQ2_PORG3	42 kDa
Uncharacterized protein	PGN_1557	B2RL31_PORG3	30 kDa
Ferric enterobactin receptor	<i>pfeA_1</i>	B2RIK7_PORG3	79 kDa

**Figure S9. Schematic representation GELNs miRNAs targeting genes in *P. gingivalis*, Related to Figure 5 and Figure 6.**

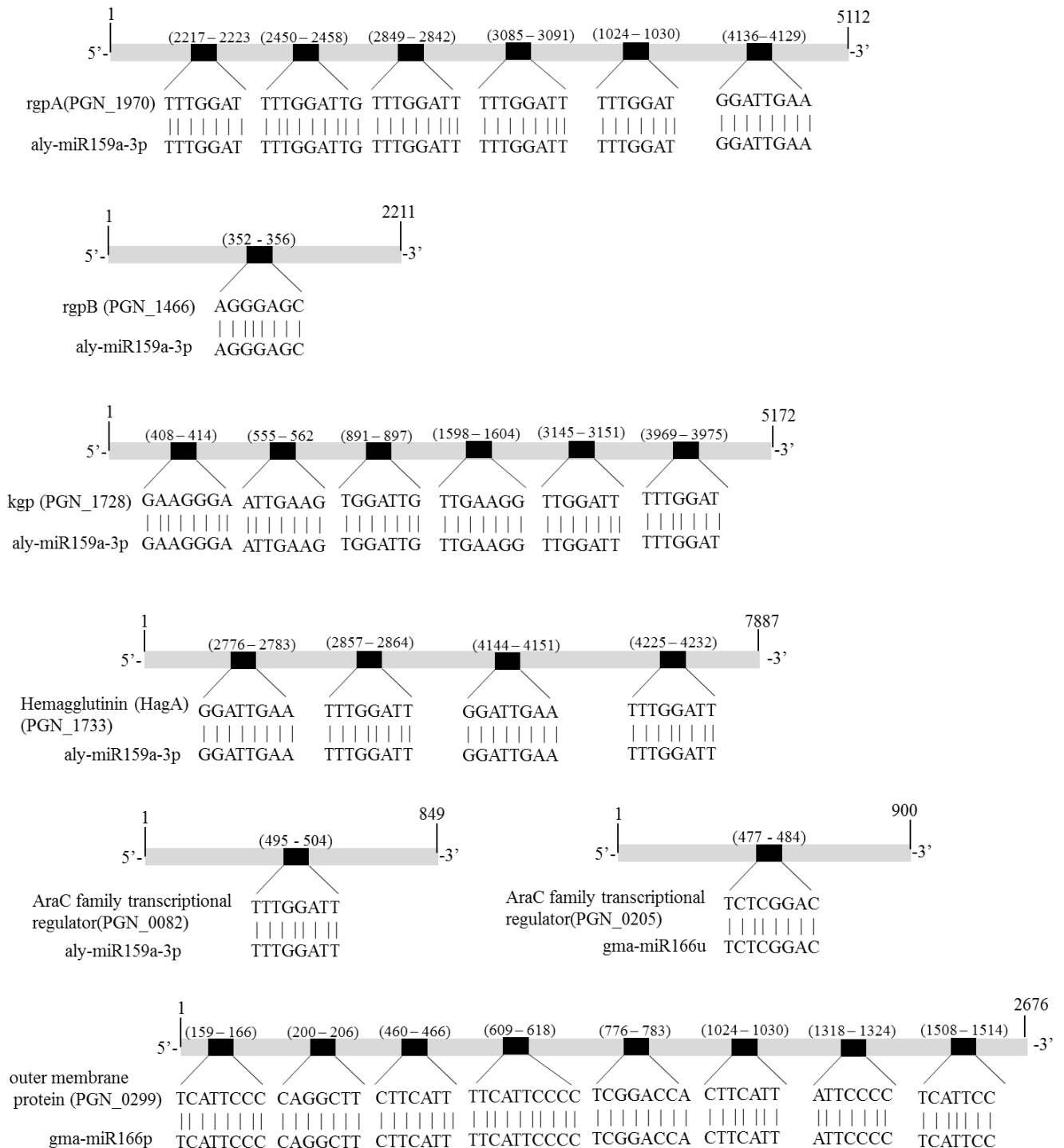
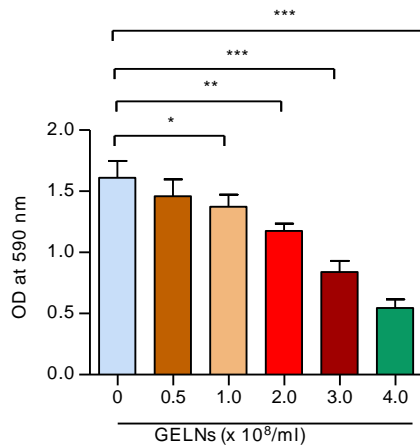
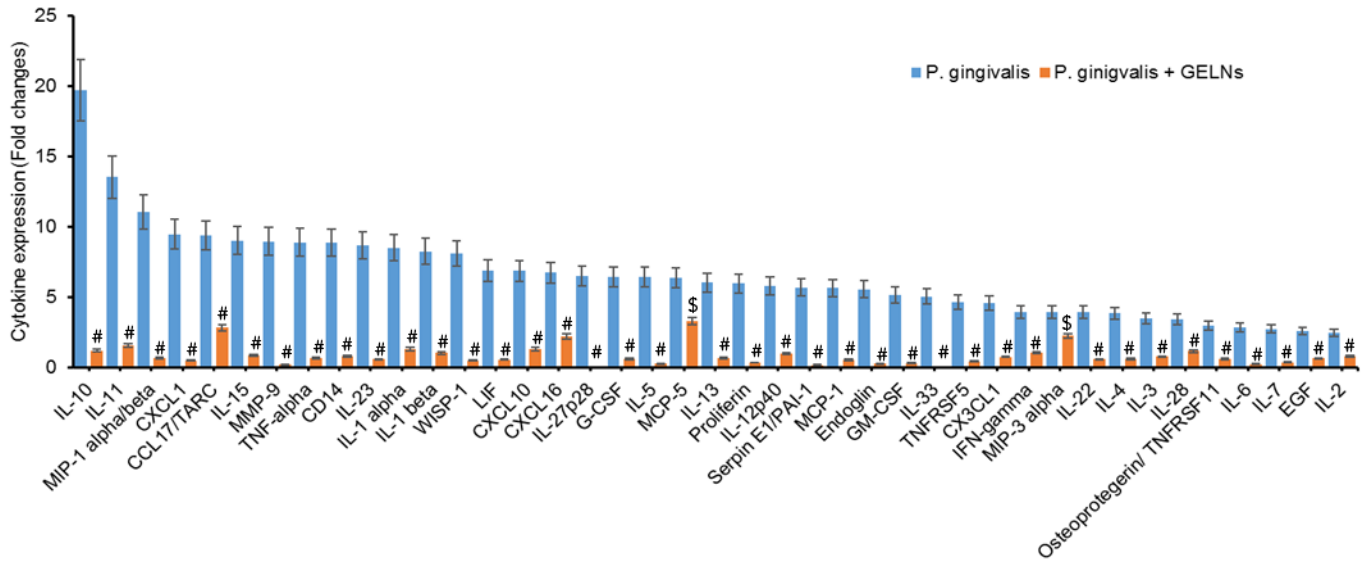


**Figure. S10. GELNS inhibit biofilm formation of *P. gingivalis*, Related to Figure 8.**



Human saliva was coated in 96-well plate for overnight. *P. gingivalis* was treated with different concentration ( $0- 4.0 \times 10^8$  particles/ml) of GELNS and incubated at anaerobic chamber for 24 h. Then, bacteria were removed by washing with PBS and the biofilm was stained with 0.5% of crystal violet for 15 min. Excess staining was removed by washing and 99% ethanol added. Optical density was measured at 590 nm. Results are expressed as means with standard deviation from three independent experiments. \*  $P < 0.05$ , \*\* $P < 0.01$ , \*\*\* $P < 0.001$  compared with control group using Student 't' Test.

**Figure S11. GELNs significantly decreased pro-inflammatory cytokine expression in *P. gingivalis* infected mice, Related to Figure 8.**



Cytokine expression was determined by a cytokine array. Plasma was collected from control, *P. gingivalis* infected and *P. gingivalis* infected with GELN treated mice. The cytokines levels are expressed as mean  $\pm$  standard deviation from three independent experiments. Student 't' test was used to analysis statistical significance of cytokine level between *P. gingivalis* infected Vs GELNs treatments. \$P<0.01, #P<0.001.

**Table S6. Primers list, Related to Figure 5, Figure 6, Figure 7 and Figure 8**

<b>Primer Name</b>	<b>Forward</b>	<b>Reverse</b>
AraC	CGCGAACTCTTCTGCATCTT	GAATACGAAGGCACGAAAGC
OMP	GGATCGTTCGCTTCAGATGT	AGCCATGATGGAAATTTTGG
RodA	CGATTATAAGGGACGGATCG	CCATCATGAAAAGGTGGGATA
HA	GATCGATGCTGATGGTGATG	CCGCTAGCAGTCCATGATTT
porX	GATCGGGGACAGAAGTACCA	ATTCGGGTAGGCGAAGAAGT
porY	AGAATTGAGGATGCCGAATG	TGCATACGAGCCTTTCTCCT
porL	GGGTGCTCTCTTCAAGTTGC	TCCATCGGATTCTTCGAGTC
porM	TTCCGTCACAGCTCAATCAG	ATTTCACGCTTACCCAAACG
porN	TCGCTCGTGAACGAGTAATG	GAATCGGGCGTAGGACAGTA
porK	AGCTCAATCCGGATCAAATG	GATGATATTGCCGCTTTCGT
porW	CTCAGTCCGGACAGGAGAAG	CTGCAGGAAATCGGCATTAT
sov	AGGCGGCAGAGACTATGAAA	CTGATAAACCTGCCCGTTGT
porQ	ATGCGTTTCCTGAACTACGG	CACCAAGGCCAAAGGAACTA
porP	AGCTACTGACGGGCACAGTT	AAAGCATAGCCGGCATAGAA
porT	GGTCTCGGATGCGATTTTTA	CTCGAAATTGAACGTGAGCA
porV	CTCTGTGCCATCGCTGAATA	AGAAACCGGTCATCTGCATC
OMPA2	CATTGACATTGCAGGTGGAG	TCGAACATGAAGTCGAGGTG
fimA	TTGTTGGGACTTGCTGCTCTTG	TTCGGCTGATTTGATGGCTTCC
16S rRNA	AGGAACTCCGATTGCGAAGG	TCGGTTTACTGCGTGGACTACC
IL-1 $\beta$	GTTCCCATTAGACAACCTGC	GATTCTTTCCTTTGAGGC
IL-6	GATACCACTCCCAACAGACC	GCAATGGCAATTCTGATTGT
TNF- $\alpha$	TCTATGGCCCAGACCCTCAC	GACGGCAGAGAGGAGGTTGA
GAPDH	AGGTCATCCCAGAGCTGAACG	ACCCTGTTGCTGTAGCCGTAT

## Transparent Methods

### Bacterial strains and growth condition

*P. gingivalis* 33277 was cultured in trypticase soy broth supplemented with yeast extract (1 mg/ml), hemin (5 µg/ml) and menadione (1 µg/ml) and incubated at 37°C in an anaerobic chamber (85%N<sub>2</sub>, 10%H<sub>2</sub>, 5%CO<sub>2</sub>). *S. gordonii* DL1 was cultured in brain-heart infusion broth containing 0.5% yeast extract and incubated anaerobically at 37°C.

A *P. gingivalis* 33277 deletion mutation in *HBP35* (PGN\_0659) was obtained by allelic replacement. Briefly, DNA sequences 999 bp upstream of the PGN\_0659 ATG initiation codon and 930 bp downstream of the PGN\_0659 TGA stop codon were amplified using the 0659usF-GATGAGCCGACGATGAGTATGC, 0659usR  
GAAGCTATCGGGGTACCTTGCAAATACTTTGCCTCTGTTATCGTC and 0659dsF  
TGTCCCTGAAAATTTTCATCCTATTGAGCTAAGATTTAAACGAAAACACTGCG, 0659dsR  
AATGCTCGGTTTCAGTGTCTGC primers, respectively, using *P. gingivalis* 33277 genomic DNA.

An *ermF* cassette was amplified from *P. gingivalis* 33277Δ*ltp1* as described earlier (Simionato et al., 2006) using the *ermF* GGTTACCCCGATAGCTTCC and *ermR* GGATGAAATTTTTCAGGGACA primers that contained 5' homology with the 0659usR and 0659dsF primers. The final PCR fusion product was purified using the New England Biolabs Monarch PCR and DNA cleanup kit. The amplicon was directly electroporated into *P. gingivalis* 33277 (Simionato et al., 2006). Recombinants were selected using TSB blood agar plates supplemented with yeast extract, hemin, menadione and erythromycin (10 µg/mL). Replacement of PGN\_0659 was confirmed by real-time PCR using the following primers 0659-F - TACTCTCTGCTGCTATCCTAAGT and 0659-R CCTCCAACACCACATTCTTCT; 0658-F- GCTTCCGGTAGCGATGATAA and 0658R- CACCTCCACATACTCGTCATAC; 0660-F- TGGCTTATCGTGGCTCTTTC and 0660-R- GGAGGATCTCTTCTGCATCAC.

To measure the effect of GELNs on growth, *P. gingivalis* and *S. gordonii* were cultured over 0-48 h in the presence or absence of different concentrations of GELNs (0-6.0 × 10<sup>8</sup> particles/ml) and

total lipids derived from these particles (LipdG) (see below). *P. gingivalis* and *S. gordonii* growth was determined by measuring optical density at 600 nm.

### **Culture of TIGK cells**

Human telomerase immortalized keratinocytes (TIGKs) derived from the human gingival epithelium were maintained at 37°C and 5% CO<sub>2</sub> in Dermalife-K serum free culture medium (Lifeline Cell Technology, Carlsbad, CA).

### **Isolation and purification of ginger exosome-like nanoparticles (GELNs)**

Ginger exosome-like nanoparticles (GELNs) were isolated and purified. Ginger was purchased from a local supermarket and washed with sterile PBS and the skin peeled away. Ginger was ground in a blender to obtain the juice and strained to remove the larger particles. Juice was sequentially centrifuged at 1000g for 10 min, 3000g for 20 min and 10,000g for 40 min to remove particles. The supernatant was then centrifuged at 150,000g for 2 h, the pellet was resuspended in sterile PBS and transferred to a sucrose step gradient (8%/15%/30%/45%/60%), followed by centrifugation at 150,000g for 2 h at 4°. The bands between the 8%/30% layer and 30%/45% layer were harvested separately and noted as ginger exosome-like nanoparticles (GELNs). The purified GELNs were fixed with 2% paraformaldehyde and imaged by electron microscopy (Zeiss EM 900). GELN size and concentration (particle number) was determined using a NanoSight NS300 (Malvern Instrument, UK) at a flow rate of 30 µl per minute. GELNs were also isolated from a commercially available ginger supplement (Super pure Ginger, The Synergy Company) after ginger supplement was suspended in PBS with the same procedure as described above.

### **GELN uptake assay**

Bacterial uptake of GELNs was quantified by flow cytometry. In brief, *P. gingivalis* and *S. gordonii* were labelled with PKH67 (green) and GELNs were labelled with PKH26 (red) according to the manufacturer's protocol (Sigma). Fluorescent labeled bacteria ( $1 \times 10^8$ ) were incubated with fluorescent labeled GELNs ( $0-6.0 \times 10^8$  particles) for 1 h at 37°C in an anaerobic chamber. The percentage of GELNs taken up by *P. gingivalis* or *S. gordonii* was quantified by flow cytometry.

### **Confocal microscopy**

The interaction or uptake of GELNs by *P. gingivalis* was determined by confocal microscopy. Briefly, *P. gingivalis* and GELNs were labelled with PKH67 (green) and PKH26 (red), respectively, according to the manufacturer's protocol (Sigma). Fluorescent labeled *P. gingivalis* ( $1 \times 10^8$ ) was incubated with fluorescent labeled GELNs ( $6.0 \times 10^8$  particles) for 1 h at 37°C. The interaction of *P. gingivalis* and GELNs was visualized by confocal microscopy (Nikon).

### ***P. gingivalis* invasion of epithelial cells**

*P. gingivalis* invasion into oral epithelial cells was determined by an antibiotic protection assay. *P. gingivalis* was grown to mid-log phase and incubated at 37°C for 3 h with or without GELNs ( $4.0 \times 10^8$  particles). Cells were collected by centrifugation for 10 min at 5000g and infected into TIGK cells at a MOI of 10 at 37°C for 1 h. Unbound bacteria were removed by washing with PBS and surface attached external non-invading bacteria were killed by incubation with gentamicin (300 µg/ml) and metronidazole (200 µg/ml) for 4 h. TIGK cells were washed with PBS and lysed with sterile distilled water. Intracellular *P. gingivalis* were plated, incubated anaerobically at 37°C for 7 days and CFUs determined. For the proliferation assay, after antibiotic treatment, cells were further incubated anaerobically for 24 h. RNA was extracted and subjected to real time PCR for 16s rRNA expression. The number of *P. gingivalis* was calculated using a standard curve derived from a known amount of *P. gingivalis*.

### ***P. gingivalis* attachment to epithelial cells**

The amount of *P. gingivalis* attaching to the surface of gingival epithelial cells was determined. TIGK cells were cultured in 96-well plates for 24 h and fixed with 5% buffered formalin for 1 h, *P. gingivalis* treated with and without GELNs (as above) were reacted with the TIGK cells at a MOI of 10 for 1 h at 37°C. Cells were washed with PBS to remove non-adherent bacteria and incubated with *P. gingivalis* whole-cell antibodies (1:10,000) for 1 h at 37°C. After washing, binding was detected with a secondary horse radish peroxidase (HRP)-anti-rabbit antibody (1:5,000) with 3,3',5,5'-tetramethylbenzidine substrate (Sigma), and the results at 450 nm recorded.

For confocal microscopy, the secondary antibody for *P. gingivalis* was Alexa 568-conjugated IgG (1: 5000). Nuclear staining was performed with DAPI for 15 min and localization of *P. gingivalis* was visualized by confocal microscopy (Nikon).



### **Gingipain proteolytic activity**

The proteolytic activity of arginine-specific (Rgp) and lysine specific (Kgp) gingipain was measured. *P. gingivalis* was cultured to mid-log phase and treated with and without GELNs ( $2.0\text{--}4.0 \times 10^8$  particles /ml) for 6 h. The bacterial cells were collected by centrifugation at 5000g for 10 min, washed and lysed with Bugbuster reagent (Millipore Sigma, Burlington, MA, USA). The chromogenic *p*-nitroanillide substrates N-benzoyl-L-arginine-pNA or toluenesulfonyl-glycyl-prolyl-L-lysine-pNA (Sigma) were used to measure RgpA/B and Kgp, respectively. Bacterial cell lysates (50  $\mu$ l) were pre-incubated with assay buffer (200 mM Tris-HCl, 5 mM CaCl<sub>2</sub>, 150 mM NaCl and supplemented with 10 mM cysteine) in a 96-well plate and 0.5 mM of specific substrate was added to each well. The rate of substrate hydrolysis and accumulation of *p*-nitroanillide was monitored spectrophotometrically at 405 nm. The enzyme activity was calculated and given as mOD/min/ $\mu$ l.

### **RNA isolation and quantitative real time PCR (qRT-PCR)**

Total RNA was isolated from *P. gingivalis* and TIGK cells using TRIzol reagent according to the manufacturer's protocol (Invitrogen). RNA (1  $\mu$ g) was converted into cDNA with an iScript cDNA synthesis kit (Bio-Rad, Hercules, CA). cDNA samples were amplified with Sso Fast green super mix in CFX96 Real-time PCR system (Bio-Rad). mRNA expression was quantified by the  $\Delta\Delta$ Ct method using 16 S rRNA expression as an internal control for bacterial gene expression and GAPDH expression as an internal control for mouse and human gene expression. All primers were purchased from Eurofins MWG Operon and primers are listed in Supplementary Table 6.

### **Western blot**

*P. gingivalis* was incubated anaerobically at 37°C for 6 h with or without GELNs ( $0\text{--}4.0 \times 10^8$  particles /ml). Total cell lysates were prepared in Bugbuster lysis reagent with protease and phosphatase inhibitors (Roche). Cell lysates were separated by SDS-PAGE (4- 15% gradient gel) and transferred onto nitrocellulose membranes. After transfer, membranes were probed with primary polyclonal antibodies specific for FimA or Mfa1 at 1:1000 for 1 h at room temperature. The membrane was incubated with secondary antibodies conjugated to Alex-647 (Eugene, OR, USA) at 1:10,000 for 1 h at room temperature. Bands were visualized and analyzed based on band intensity on an Odyssey Imager (Licor Inc, Lincoln, NE, USA).

### **Lipid extraction and TLC analysis**

Total lipids from GELNs were extracted with chloroform:methanol (2:1, v/v). GELNs were mixed with chloroform:methanol and vortex the mixture. Centrifuge at 2000 xg for 10 min and carefully remove bottom layer contains lipids and dried under nitrogen. Then, thin layer chromatography (TLC) was performed. HPTLC-plates (silica gel 60 with concentrating zone, 20 cm x 10 cm; Merck) were used for the separation. Aliquots of concentrated lipid samples extracted from GELNs were separated on HPTLC-plates and the plates developed with chloroform:methanol:H<sub>2</sub>O (65:25:4). After drying, lipids were stained using iodine vapor. The plate was imaged with an Odyssey Scanner.

**Lipid oxidation measurement:** Lipid oxidation was measured by quantification of malondialdehyde (MDA) 200 µl of lipids derived from GELNs and GELN lipids extracted from TLC plates were mixed with 400 µl of TBA reagent containing Trichloroacetic acid (15%), HCl (0.2N), thiobarbituric acid (0.37%) with 0.03% butylated hydroxytoluene (BHT). The sample was kept in boiling water bath for 15 min and samples cooled down to room temperature. The samples were centrifuged for 10 min at 1000g. The absorbance of the solution at 535 nm was determined. The concentration of MDA was calculated using standard MDA.

### **Lipidomic analysis**

Lipid samples extracted from GELNs were submitted to the Lipidomics Research Center, Kansas State University (Manhattan, KS) for analysis. The lipid composition was determined using a triple quadrupole mass spectrometer (Applied Biosystems Q-TRAP, Applied Biosystems, Foster City, CA). The data are reported as concentration (nmol/mg GELNs) and percentage of each lipid in total signal for the molecular species determined after normalization of the signals to internal standards of the same lipid class.

### **Preparation of GELN RNA libraries and sequencing**

Small RNA libraries were generated with 100 ng of total RNA from GELNs and TruSeq Small RNA Library Preparation Kits (Illumina) according to the manufacturer's instructions. Following PCR amplification (16 cycles), libraries between 140 and 160 bp in size were gel purified and resuspended in ultrapure water (11 µl). Equal amounts of libraries were pooled and sequenced

on an Illumina HiSeq 2500, followed by demultiplexing and fastq generation with CASAVA v1.8.4. Raw fastqs were adapter and quality score trimmed with cut adapt v1.10. with a minimum length of 15 nucleotides. MicroRNAs were identified using the sRNABench Pipeline (version 05/14). A core set of plant miRNAs from miRBase v21 was used as a reference and this set included all 14 plant species with at least 200 mature microRNA sequences annotated in miRBase. Within the sRNABench pipeline, mapping was performed with bowtie (v0.12.9) and microRNA folding was predicted with RNAfold using the Vienna package (v2.1.6).

### **Delivery of miRNA into *P. gingivalis***

GELNs miRNAs aly-miR-159a-3p, gma-miR166u, gma-miR166p and gma-miR319a were packaged into lemon-derived lipid nanoparticles. Total lipids were extracted from lemon-derived exosome-like nanoparticles. 20 nM of miRNA was added to 100 nM of lemon lipids in 0.9% NaCl and PEI (2 µg/ml), and this mixture was sonicated in a water bath to make a lipid nanoparticles-miRNA complex. The complex was centrifuged at 36,000 rpm for 1 h and the unbound RNA content in the supernatant was measured. *P. gingivalis* was treated with the RNA bound lipid nanoparticles for 24 h.

### **2DLC-MS/MS analysis and its data analysis**

*P. gingivalis* was incubated anaerobically with PBS in the presence or absence of GELNs ( $4.0 \times 10^8$  particles/ml) for 24 h. Bacterial media was collected by centrifugation and filtered (0.22 µm) to remove bacterial cells. To extract polar metabolites for 2DLC-MS/MS analysis, 500 µL of culture medium was lyophilized, then redissolved in 100 µL 20% acetonitrile. After 3 min of vigorous vortex mixing, the sample was centrifuged at 12,000g at 4°C for 20 min. The supernatant was collected and used for 2DLC-MS/MS analysis.

All samples were analyzed on a Thermo Q Exactive HF Hybrid Quadrupole-Orbitrap Mass Spectrometer coupled with a Thermo DIONEX UltiMate 3000 HPLC system (Thermo Fisher Scientific, Waltham, MA, USA). The UltiMate 3000 HPLC system was equipped with a hydrophilic interaction chromatography (HILIC) column and a reverse phase chromatography (RPC) column. The HILIC column was a SeQuant® ZIC®-cHILIC HPLC column (150 × 2.1 mm i.d., 3 µm) purchased from Phenomenex (Torrance, CA, USA). The RPC column was an ACQUITY UPLC

HSS T3 column (150 × 2.1 mm i.d., 1.8 μm) purchased from Waters (Milford, MA, USA). The two columns were configured in parallel 2DLC mode.

For 2DLC separation, the mobile phase A for RPC was water with 0.1% formic acid and the mobile phase A for HILIC was 10 mM ammonium acetate (pH adjusted to 3.25 with acetate). Both RPC and HILIC used the same mobile phase B, acetonitrile with 0.1% formic acid. The RPC gradient was 0 min, 5% B, hold for 5.0 min; 5.0 min to 6.1 min, 5% B to 15% B; 6.1 min to 10.0 min, 15% B to 60% B, hold for 2.0 min; 12.0 min to 14.0 min, 60% B to 100% B, hold for 13.0 min; 27.0 min to 27.1 min, 100% B to 5% B, hold for 12.9 min. The HILIC gradient was 0 to 5.0 min, 95% B to 35% B, hold for 1.0 min; 6.0 min to 6.1 min, 35% B to 5% B, hold for 16.9 min; 23.0 min to 23.1 min, 5% B to 95% B, hold for 16.9 min. The flow rate was 0.4 mL/min for RPC and 0.3 mL/min for HILIC. The column temperature was 40°C for both columns. The injection volume was 2 μL.

To avoid systemic bias, the samples were analyzed by 2DLC-MS in a random order. All samples were first analyzed by 2DLC-MS in positive mode followed by 2DLC-MS in negative mode to obtain the full MS data of each metabolite. For quality control purposes, a pooled sample was prepared by mixing a small portion of the supernatant from each sample and was analyzed by 2DLC-MS after injection of every six biological samples. The pooled sample was also analyzed by 2DLC-MS/MS in positive mode and negative mode to acquire MS/MS spectra for metabolite identification.

For 2DLC-MS data analysis, MetSign software was used for spectrum deconvolution, metabolite identification, cross-sample peak list alignment, normalization, and statistical analysis. To identify metabolites, the 2DLC-MS/MS data of pooled sample were first matched to our in-house MS/MS database that contains the parent ion  $m/z$ , MS/MS spectra, and retention time of 187 metabolite standards. The thresholds used for metabolite identification were MS/MS spectral similarity  $\geq 0.4$ , retention time difference  $\leq 0.15$  min, and  $m/z$  variation  $\leq 4$  ppm. The 2DLC-MS/MS data without a match in the in-house database were then analyzed using Compound Discoverer software (Thermo Fisher Scientific, Inc., Germany), where the threshold of MS/MS spectra similarity score was set as  $\geq 40$  with a maximum score of 100. The remaining peaks that did not

have a match were then matched to the metabolites in our in-house MS database using the parent ion m/z and retention time. The thresholds for assignment using the parent ion m/z and retention time were  $\leq 4$  ppm and  $\leq 0.15$  min, respectively.

### **Transmission Electron Microscopy**

*P. gingivalis* and *S. gordonii* were treated with PBS or GELNs ( $6.0 \times 10^8$  particles/ml) for 3 h. Bacterial cells were collected by centrifugation (5000 g, 10 min) and resuspended in 10 mM Tris (pH7.8) and fixed with 2% formaldehyde and 1% glutaraldehyde. The bacterial suspension (20  $\mu$ l) was applied to a formvar-coated copper grid (200 mesh, Electron Microscopy Science, PA), air dried and negatively stained with 0.5% ammonium molybdate. Bacterial morphology was observed with a transmission electron microscope (Thermo-Fisher TEM Tecnai Spirit) at 80 kV and images were collected with an AMT XR60 digital camera.

### **Outer membrane permeability assay (EtBr influx assay)**

*P. gingivalis* was grown to mid-log phase and washed with binding buffer (25 mM MES pH 6.0, 25 mM NaCl). *P. gingivalis* was treated for 2 h at 37°C with or without GELNs ( $0-6.0 \times 10^8$  particles/ml) and then ethidium bromide (0.5  $\mu$ M) was added. The fluorescence of the Et-Br-nucleic acid complex was immediately measured in a fluorescence spectrophotometer (Molecular Device) with excitation and emission wavelengths of 545 and 600 nm, respectively. The widths of the slits were 5 and 10 nm, respectively.

### **Cytoplasmic membrane integrity assay**

The cytoplasmic membrane depolarization of *P. gingivalis* was measured by using a membrane potential sensitive fluorescent dye diSC<sub>3-5</sub>. Mid-logarithmic phase *P. gingivalis* was washed with 5 mM sodium HEPES buffer, pH 7.4, containing 20 mM glucose, and resuspended to an OD<sub>600</sub> of 0.05 in the same buffer. The cell suspension was incubated with 0.4  $\mu$ M diSC<sub>3</sub> until a stable reduction of fluorescence was achieved. KCl was added to a final concentration of 0.1 M to equilibrate the cytoplasmic and external K<sup>+</sup> concentration. *P. gingivalis* was treated for 2 h at 37°C with or without GELNs ( $6.0 \times 10^8$  particles /ml). Changes in fluorescence were recorded using an F-4500 fluorescence spectrophotometer (Hitachi, Japan) with an excitation wavelength of 622 nm and an emission wavelength of 670 nm.

### **Lipid nanoparticles preparation**

Total GELN lipids were extracted with chloroform:methanol (2:1, v/v) Thin layer chromatography (TLC) was performed with a PA (34:2) standard. The corresponding PA band was excised from the TLC plate and the remaining bands were pooled together. GELN total lipids, PA depleted lipids and PA (34:2) were completely dried under a stream of nitrogen gas and overnight dry under vacuum. The lipid film was suspended in HBS running buffer (20 mM HEPES, 150 mM NaCl, pH 7.4), gently vortexed and sonicated for 10 min until a clear solution was formed. The lipid nanoparticle suspension was extruded through a polycarbonate membrane filter syringe with a pore size of 100 nm. The size of the lipid nanoparticles was confirmed using a NanoSight NS300 (Malvern Panalytical Inc, MA, USA). Total lipids were determined by measuring total phosphate level (Baginski et al., 1972).

### **HPLC analysis of TAG**

Total lipids were extracted from GELNs and lipid nanopartilces made from GELNs lipid. The samples were dissolved in methanol and 10  $\mu$ l of sample was injected for high-performance liquid chromatography (HPLC) analysis with 380 ELSD detection system (Agilent Technologies). The HPLC analysis was performed on an Agilent 1260 Infinity system equipped with an Agilent 300SB-C8 column (4.6 x 250 mm, 5  $\mu$ m) connected to a guard column, with the following parameters: mobile phase A: water; mobile phase B: methanol; gradient: 10% B in first 5 min, increase to 95% B in 10 min, hold 95% B for 5 min and then back to 10 % B in 5 min; flow rate: 1.0 ml/min; Column temperature was controlled at 37°C. ELSD setting include evaporator temperature 30°C, nebulizer temperature 30°C, gas flow rate 1.2 SLM and 350 kPa for nitrogen pressure with flow rate was 1 ml/min. The standard glyceryl trinoleate (cat: T9517) was purchase from Sigma.

### **Surface Plasmon Resonance (SPR)**

SPR experiments were conducted on an OpenSPR™ (Nicoya, Lifesciences, ON, CA). All experiments were performed on a LIP-1 sensor (Nicoya, Lifesciences). Tests were run at a flow rate of 20  $\mu$ l/min using HBS running buffer (20 mM HEPES, 150 mM NaCl, pH 7.4). First, the LIP-1 sensor chip was cleaned with octyl  $\beta$ -D-glucopyranoside (40 mM) and CHAPS (20 mM). Liposomes (1 mg/ml) were injected on the sensor chip for 10 min until stable resonance was

obtained. After immobilization of lipid nanoparticles, the surface was blocked with BSA (3%) in running buffer. After a stable signal was obtained, *P. gingivalis* total cell lysates (5 µg/ml of protein) were run over the immobilized liposomes. A negative control test was also performed by injecting protein onto a blank sensor chip to check for non-specific binding. After 10 min, the lipid nanoparticle binding protein was eluted using NaOH (200 µM). The eluted protein was subjected to LC-MS proteomic analysis for identification of GELN lipid nanoparticles and PA binding proteins. The sensograms were analyzed using TraceDrawer kinetic analysis software.

### **Lipid nanoparticle pull down assay**

GELN lipid interactions with HBP35 were further confirmed using a lipid nanoparticle pull down assay. GELN lipid nanoparticles were fluorescently labelled with PKH26 in vesicle buffer (50 mM Tris-HCl (pH 7.5) and 150 mM NaCl). The labelled nanoparticles were incubated with biotin-HBP35 peptide (100 µM) for 2 h at 4°C with rotation in vesicle buffer. The lipid-protein complex was pulled down by streptavidin magnetic beads. The complex was washed thoroughly and the presence of lipid nanoparticles in the complex confirmed by flow cytometer. The number of lipid nanoparticles in the complex was determined using a Nanosight 300 and the quantity of lipid nanoparticles was determined by fluorescence intensity measured in a fluorescence spectrophotometer (Molecular Device) with excitation and emission wavelengths of 551 and 567 nm, respectively.

### **Proteomic sample preparation**

GELN binding proteins of *P. gingivalis* were identified by LC-MS proteomics. Briefly, GELNs were labelled with biotin using an EZ-Link™ Sulfo-NHS-Biotinylation Kit according to the manufacturer's protocol (Thermo Fisher Scientific, San Jose, CA, USA). Biotin labelled GELNs were incubated with *P. gingivalis* for 1 h at room temperature with rotation. Biotin was pulled down by streptavidin magnetic beads (Thermo Fisher Scientific) and the beads were washed thoroughly with PBS to remove unbound protein. The protein bound magnetic beads were suspended in lysis buffer (2% SDS, 100 mM DTT, 20 mM Tris-HCl pH 8.8) at 95°C for 20 min. Protein was collected from supernatants after centrifugation and the concentration estimated using a Protein Assay Kit (Bio-Rad, Hercules, CA, USA). Protein aliquots (50 µg) were diluted into 4% SDS / 0.1M Tris-HCl

pH8.5 and 1M DTT and were processed according to the filter-aided sample preparation (FASP) method as described (Teng et al., 2017). The digested, ultra-filtered samples were trap-cleaned with C18 PROTO™, 300Å Ultra MicroSpin columns, lyophilized by vacuum centrifugation, re-dissolved into 16 µl of 2% v/v acetonitrile, and concentrations estimated based on absorption at 205 nm using a Nanodrop 2000 (Thermo Fisher Scientific).

### **Liquid chromatography–mass spectrometry (LC-MS) data analysis**

Proteome Discoverer v1.4.1.114 (Thermo Fisher Scientific,) was used to analyze the data collected by the mass spectrometer. The database used in Mascot v2.5.1 and SequestHT searches was the 2/17/2017 version of the *P. gingivalis* proteome from UniprotKB (Proteome ID UP000236566). Scaffold was used to calculate the false discovery rate using the Peptide and Protein Prophet algorithms. Proteins were grouped to satisfy the parsimony principle. The proteins were clustered based on differential expression and heat maps representing differentially regulated proteins by GELNs were generated using software R.

### **Monotypic biofilm assay.**

*P. gingivalis* biofilm was quantified using a microtiter plate assay. Saliva was collected in a sterile centrifuge tube on ice from healthy donors. DTT was added to a 2.5 mM final concentration, then centrifuged at 5,000 g for 10 min at 4°C. The clarified saliva supernatant was transferred, and 3 volumes of sterile distilled water added, and the 25% saliva was filtered through a 0.22 µm pore size filter. 96-well polystyrene cultured plate (Corning Inc., Corning, NY) was pre-coated with 25% saliva and incubated at 37°C for overnight. *P. gingivalis* strains were grown to mid-log phase ( $OD_{600} = 0.8$ ) and aliquots (200 µl) of samples were anaerobically incubated in the 25% saliva-coated wells with and without ginger exosomes like nano particles ( $4.0 \times 10^8$  particles/ml) for 24 h. A sample (100 µl) of each cell culture was measured by optical density at 600 nm to assess planktonic bacterial growth. After discarding the planktonic bacterial cells in the wells, bacterial cells bound to the wells were gently washed three times with PBS, air dried, and then stained with 200 µl of 1% (w/v) crystal violet for 15 min. After washing twice with PBS and then with sterile



water to remove excess dye, the cell-bound dye was eluted using 200 µl of 95% ethanol. The absorbance was measured at 540 nm using 96-well plate reader (Molecular device).

### **Animal infection**

Animal infection with *P. gingivalis* was carried out as described previously (Kuboniwa et al., 2017). Female 10-12-week-old C57BL/6 mice were obtained from Jackson Laboratories, maintained in groups and housed in micro isolator cages. Mice were fed a standard diet with water *ad libitum* and kept on a 12 h light and dark cycle. Animal care was performed following the Institute for Laboratory Animal Research (ILAR) guidelines and all animal experiments were done in accordance with protocols approved by the University of Louisville Institutional Animal Care and Use Committee (Louisville, KY). Before oral inoculation, mice were initially treated with sulfamethoxazole (800 µg/ml) and trimethoprim (400 µg/ml) *ad libitum* in water for ten days at two-day intervals. The mice were divided into four groups (five animals per group): control (uninfected) provided regular water, *P. gingivalis* infected provided regular water, *P. gingivalis* infected and provided GELNs containing water, control (uninfected) provided GELNs in water. *P. gingivalis* was suspended in 1 ml of 2% carboxymethylcellulose (CMC) and orally inoculated into mice at two-day intervals over a ten-day period. Mice were given GELN ( $4.0 \times 10^8$  particles /ml) *ad libitum* in drinking water. To enumerate the colonization of *P. gingivalis*, oral samples were collected along the gingiva of the upper molars using a sterile polyester-tipped applicator at one, two and three weeks after the final bacterial infection. Total genomic DNA was isolated from these samples using a QIAamp DNA isolation kit (Qiagen) and amplified by qPCR with primers to 16s rRNA Forward 5'-AGGAACTCCGATTGCGAAGG-3' and reverse 5'-TCGTTTACTGCGTGGACTACC-3'. Numbers of *P. gingivalis* were calculated using a standard curve derived from known amounts of *P. gingivalis*. Forty-two days after the last infection, mice were euthanized and skulls were subjected to µCT scan (SKYSCAN 1174, Bruker). Bone loss was assessed by measuring the distance between the alveolar bone crest and the cemento-enamel junction at 14 predetermined points on the maxillary molars. For bone volume analysis, a region of interest (ROI) was drawn manually on the axial planes, between the medial root surface of the first molar and distal root

surface of the third molar. A three-dimensional image was generated from the ROI. All root volumes were excluded from the ROI to calculate the total volume (TV). The bone volume fraction (BV/TV) was calculated for each sample.

### **Histology and immunofluorescence staining**

Oral tissue specimens were decalcified with 0.5 M EDTA (pH 7.4) for 3-4 weeks and processed for paraffin embedding. Tissue samples were cut at 5  $\mu$ m thickness and stained with hematoxylin. For immunofluorescence analysis, tissue sections were subjected to antigen retrieval by boiling the slides in antigen unmasking solution (Vector laboratories) for 10 min according to the manufacturer's instructions. Sections were blocked with 5% BSA in PBS for 1 h at room temperature and incubated with the primary antibodies (1: 100) anti-rabbit-CD3, anti-CD45 or F4/80 at 4°C overnight. After extensive washing with PBS, tissue sections were incubated with Alexa 568-conjugated IgG and Alexa 488-conjugated IgG (1: 5000 dilution) for 1 h at room temperature. Nuclear staining was performed with DAPI for 15 min and images were captured by confocal microscopy (Nikon). To determine the number of osteoblasts, the sections were incubated with anti-rabbit-RUNX2 antibody (1:100) overnight at 4°C. HRP-conjugated anti-rabbit (1:5000) was used as secondary antibody and DAB chromogen was used as substrate. The slides were counterstained with hematoxylin. Similarly, the number of osteoclasts was determined using sections stained with TRAP (Sigma) according to manufacturer's protocol. The slides were counterstained with hematoxylin. The number of osteoblasts and multinucleated osteoclasts was counted manually.

### **Statistical analysis**

Values are shown as mean  $\pm$  SD for three independent experiments. Statistical analysis was performed with GraphPad Prism 6. Comparison of multiple experimental groups was performed using the one-way Analysis of Variance test. A *t*-test was used to compare the means of two groups. *P* values of < 0.05 were considered to be statistically significant. Appropriate sample sizes were calculated to ensure statistical significance could be determined.

### **SUPPLEMENTAL REFERENCES:**

Baginski, E.S., Epstein, E., and Zak, B. (1972). The measurement of serum total phospholipids. *Annals of clinical laboratory science* 2, 255-267.

Bender, R.A. (2012). Regulation of the histidine utilization (hut) system in bacteria. *Microbiology and molecular biology reviews : MMBR* 76, 565-584.

Christgen, S.L., and Becker, D.F. (2018). Role of Proline in Pathogen and Host Interactions. *Antioxidants & redox signaling*.

Conner, R.M., and Hansen, P.A. (1967). Effects of valine, leucine, and isoleucine on the growth of *Bacillus thuringiensis* and related bacteria. *Journal of invertebrate pathology* 9, 12-18.

Cozzone, A.J. (2005). Role of protein phosphorylation on serine/threonine and tyrosine in the virulence of bacterial pathogens. *Journal of molecular microbiology and biotechnology* 9, 198-213.

Cusumano, Z.T., and Caparon, M.G. (2015). Citrulline protects *Streptococcus pyogenes* from acid stress using the arginine deiminase pathway and the F1Fo-ATPase. *Journal of bacteriology* 197, 1288-1296.

Delavier-Klutchko, C., and Flavin, M. (1965). Role of a Bacterial Cystathionine-Beta-Cleavage Enzyme in Disulfide Decomposition. *Biochimica et biophysica acta* 99, 375-377.

Deng, X., Chen, K., Luo, G.Z., Weng, X., Ji, Q., Zhou, T., and He, C. (2015). Widespread occurrence of N6-methyladenosine in bacterial mRNA. *Nucleic acids research* 43, 6557-6567.

El Qaidi, S., Yang, J., Zhang, J.R., Metzger, D.W., and Bai, G. (2013). The vitamin B(6) biosynthesis pathway in *Streptococcus pneumoniae* is controlled by pyridoxal 5'-phosphate and the transcription factor PdxR and has an impact on ear infection. *Journal of bacteriology* 195, 2187-2196.

Ferla, M.P., and Patrick, W.M. (2014). Bacterial methionine biosynthesis. *Microbiology* 160, 1571-1584.

Fuchs, G., Boll, M., and Heider, J. (2011). Microbial degradation of aromatic compounds - from one strategy to four. *Nature reviews Microbiology* 9, 803-816.

Gillner, D.M., Becker, D.P., and Holz, R.C. (2013). Lysine biosynthesis in bacteria: a metallodesuccinylase as a potential antimicrobial target. *Journal of biological inorganic chemistry : JBIC : a publication of the Society of Biological Inorganic Chemistry* 18, 155-163.

Hammes, W., Schleifer, K.H., and Kandler, O. (1973). Mode of action of glycine on the biosynthesis of peptidoglycan. *Journal of bacteriology* 116, 1029-1053.

Hart, G.W. (1982). The role of asparagine-linked oligosaccharides in cellular recognition by thymic lymphocytes. Effects of tunicamycin on the mixed lymphocyte reaction. *The Journal of biological chemistry* 257, 151-158.

Kolodkin-Gal, I., Romero, D., Cao, S., Clardy, J., Kolter, R., and Losick, R. (2010). D-amino acids trigger biofilm disassembly. *Science* 328, 627-629.

Kuboniwa, M., Houser, J.R., Hendrickson, E.L., Wang, Q., Alghamdi, S.A., Sakanaka, A., Miller, D.P., Hutcherson, J.A., Wang, T., Beck, D.A.C., *et al.* (2017). Metabolic crosstalk regulates *Porphyromonas gingivalis* colonization and virulence during oral polymicrobial infection. *Nature microbiology* 2, 1493-1499.

Kutanovas, S., Stankeviciute, J., Urbelis, G., Tauraitė, D., Rutkiene, R., and Meskys, R. (2013). Identification and characterization of a tetramethylpyrazine catabolic pathway in *Rhodococcus jostii* TMP1. *Applied and environmental microbiology* 79, 3649-3657.

Liu, P., Zhang, H., Lv, M., Hu, M., Li, Z., Gao, C., Xu, P., and Ma, C. (2014). Enzymatic production of 5-aminovalerate from L-lysine using L-lysine monooxygenase and 5-aminovaleramidase amidohydrolase. *Scientific reports* 4, 5657.

Luo, S., and Levine, R.L. (2009). Methionine in proteins defends against oxidative stress. *FASEB journal : official publication of the Federation of American Societies for Experimental Biology* 23, 464-472.

Meadows, J.A., and Wargo, M.J. (2015). Carnitine in bacterial physiology and metabolism. *Microbiology* 161, 1161-1174.

Melander, R.J., Minvielle, M.J., and Melander, C. (2014). Controlling bacterial behavior with indole-containing natural products and derivatives. *Tetrahedron* 70, 6363-6372.

Moura, A.P., Ribeiro, C.A., Zanatta, A., Busanello, E.N., Tonin, A.M., and Wajner, M. (2012). 3-Methylcrotonylglycine disrupts mitochondrial energy homeostasis and inhibits synaptic Na<sup>(+)</sup>,K<sup>(+)</sup>-ATPase activity in brain of young rats. *Cellular and molecular neurobiology* 32, 297-307.

Muto, A., and Osawa, S. (1987). The guanine and cytosine content of genomic DNA and bacterial evolution. *Proceedings of the National Academy of Sciences of the United States of America* 84, 166-169.

Rao, D.R., and Rodwell, V.W. (1962). Metabolism of pipercolic acid in a *Pseudomonas* species. I. alpha-Aminoadipic and glutamic acids. *The Journal of biological chemistry* 237, 2232-2238.

Simionato, M.R., Tucker, C.M., Kuboniwa, M., Lamont, G., Demuth, D.R., Tribble, G.D., and Lamont, R.J. (2006). *Porphyromonas gingivalis* genes involved in community development with *Streptococcus gordonii*. *Infection and immunity* 74, 6419-6428.

Teng, Y., Ren, Y., Hu, X., Mu, J., Samykutty, A., Zhuang, X., Deng, Z., Kumar, A., Zhang, L., Merchant, M.L., *et al.* (2017). MVP-mediated exosomal sorting of miR-193a promotes colon cancer progression. *Nature communications* 8, 14448.

Viala, J.P., Meresse, S., Pocachard, B., Guilhon, A.A., Aussel, L., and Barras, F. (2011). Sensing and adaptation to low pH mediated by inducible amino acid decarboxylases in *Salmonella*. *PloS one* 6, e22397.

Wargo, M.J. (2013). Homeostasis and catabolism of choline and glycine betaine: lessons from *Pseudomonas aeruginosa*. *Applied and environmental microbiology* 79, 2112-2120.

Xiong, L., Teng, J.L., Botelho, M.G., Lo, R.C., Lau, S.K., and Woo, P.C. (2016). Arginine Metabolism in Bacterial Pathogenesis and Cancer Therapy. *International journal of molecular sciences* 17, 363.